中国光学（中英文） Chinese Optics 核心期刊

双包层掺铥光纤放大器中的受激布里渊散射

刘庆敏 孙慧杰 侯尚林 雷景丽 武刚 晏祖勇

Stimulated brillouin scattering in double-clad thulium-doped fiber amplifier

LIU Qing-min, SUN Hui-jie, HOU Shang-lin, LEI Jing-li, WU Gang, YAN Zu-yong

引用本文:
刘庆敏, 孙慧杰, 侯尚林, 雷景丽, 武刚, 晏祖勇. 双包层掺铥光纤放大器中的受激布里渊散射[J]. 中国光学, 2024, 17(1): 226–237. doi: 10.37188/CO.EN–2023–0011
LIU Qing-min, SUN Hui-jie, HOU Shang-lin, LEI Jing-li, WU Gang, YAN Zu-yong. Stimulated brillouin scattering in double-clad thulium-doped fiber amplifier[J]. *Chinese Optics*, 2024, 17(1): 226-237. doi: 10.37188/CO.EN-2023-0011

在线阅读 View online: https://doi.org/10.37188/CO.EN–2023–0011

您可能感兴趣的其他文章

Articles you may be interested in

中红外波段As_2S_3光子晶体光纤中受激布里渊散射的研究

Investigation of stimulated Brillouin scattering in As_2S_3 photonic crystal fibers at the mid–infrared waveband

中国光学（中英文）. 2022, 15(4): 835 https://doi.org/10.37188/CO.EN.2022–0003

2–μm MOPA结构全光纤激光器输出特性研究

Output characteristics of an all–fiber laser with a 2–μm MOPA structure

中国光学（中英文）. 2023, 16(2): 399 https://doi.org/10.37188/CO.2022–0191

大能量碟片激光多通放大器腔体设计研究综述

Review of the cavity–design of high–energy thin–disk laser multi–pass amplifiers

中国光学（中英文）. 2023, 16(5): 996 https://doi.org/10.37188/CO.2023–0009

基于布里渊光纤振荡器的可调谐窄带微波光子滤波器研究

Tunable narrowband microwave photonic filter based on brillouin fiber oscillator

中国光学（中英文）. 2022, 15(4): 660 https://doi.org/10.37188/CO.2022–0057

单片集成式主振荡功率放大器研究进展

Research progress of monolithic integration master–oscillation power–amplifiers

中国光学（中英文）. 2023, 16(1): 61 https://doi.org/10.37188/CO.2022–0022

5.2 W高重频257 nm深紫外皮秒激光器

High repetition frequency 257 nm deep ultraviolet picosecond laser with 5.2 W output power

中国光学（中英文）. 2023, 16(6): 1318 https://doi.org/10.37188/CO.2023–0026

文章编号　2097-1842(2024)01-0226-12

Stimulated brillouin scattering in double-clad thulium-doped fiber amplifier

LIU Qing-min[1,2], SUN Hui-jie[2], HOU Shang-lin[1,2 *], LEI Jing-li[2], WU Gang[2], YAN Zu-yong[2]
（1. *College of Electrical and Information Engineering*, *Lanzhou University of Technology*, *Lanzhou* 730050, *China*;
2. *School of Science*, *Lanzhou University of Technology*, *Lanzhou* 730050, *China*）
∗ *Corresponding author*, *E-mail*: *houshanglin@vip.*163*.com*

Abstract: In this paper, the effect of Stimulated Brillouin Scattering(SBS) on the laser output performance in a 2 μm thulium-doped fiber amplifier was analyzed theoretically. The optical mode distribution, the effective refractive index, the effective mode field area, and the normalized frequency of the double-clad thulium-doped fiber at 793 nm pump wavelength and 1.9−2.1 μm laser waveband were studied. The stimulated Brillouin scattering characteristics, including the Brillouin frequency shift and the Brillouin gain spectrum, in the double-clad thulium-doped fiber were numerically simulated in the laser waveband of 1.9−2.1 μm. The influence of stimulated Brillouin scattering on the laser output performance of thulium-doped fiber amplifiers was investigated using the theoretical model of stimulated Brillouin scattering in gain fibers. In the DTDF-10/130 double-clad thulium-doped fiber, a continuous wave with power of 100 W and wavelength of 793 nm is used as a pump to amplify a continuous signal wave with wavelength of 2 μm and power of 0.01 W. The maximum output powers of the signal wave are 25.27 W, 31.08 W and 34.06 W when the pump power filling factors are 0.01, 0.02 and 0.03, respectively. The corresponding optimal double-clad fiber lengths are 2.66 m, 2.02 m and 1.75 m. Additionally, the Stokes optical powers generated by the stimulated Brillouin scattering are 1.68 W, 1.39 W and 1.14 W, respectively. The results show that the double-clad fiber with large pump power filling factor in the thulium-doped fiber amplifier can effectively reduce the fiber length, thus to minimize the influence of stimulated Brillouin scattering on the output power of the signal laser. The numerical model can optimize the fiber length of the fiber amplifier, which is of great significance to improve experimental efficiency and reduce experimental costs.

Key words: stimulated brillouin scattering; double-clad; thulium-doped fiber; amplifier

收稿日期:2023-05-16; **修订日期**:2023-05-29
基金项目:国家自然科学基金(No. 61665005);兰州理工大学红柳一流学科发展计划资助项目
Supported by National Natural Science Foundation of China (No. 61665005); HongLiu First-class Disciplines Development Program of Lanzhou University of Technology

双包层掺铥光纤放大器中的受激布里渊散射

刘庆敏[1,2], 孙慧杰[2], 侯尚林[1,2*], 雷景丽[2], 武　刚[2], 晏祖勇[2]
（1. 兰州理工大学 电气工程与信息工程学院, 甘肃 兰州 730050;
2. 兰州理工大学 理学院, 甘肃 兰州 730050）

摘要: 理论分析了波长为 2 μm 的掺铥光纤放大器中受激布里渊散射(SBS)对激光输出性能的影响, 研究了双包层掺铥光纤在 793 nm 的泵浦波长和 1.9~2.1 μm 的激光工作波段的光模分布、有效折射率、有效模场面积和归一化频率, 数值计算了在 1.9~2.1μm 的激光工作波段双包层掺铥光纤中的布里渊频移和布里渊增益谱等 SBS 特性。利用增益光纤中的受激布里渊散射理论模型, 研究了受激布里渊散射对掺铥光纤放大器激光输出性能的影响。在 DTDF-10/130 双包层掺铥光纤中, 使用功率为 100 W、波长为 793 nm 的连续光作为泵浦, 可对波长为 2 μm、功率为 0.01 W 的连续信号光进行放大。当泵浦光功率填充因子为 0.01、0.02 和 0.03 时, 信号光的最大输出功率分别为 25.27 W、31.08 W 和 34.06 W。对应的最佳双包层光纤长度为 2.66 m、2.02 m 和 1.75 m, 由受激布里渊散射产生的斯托克斯光功率分别为 1.68 W、1.39 W 和 1.14 W。结果表明, 在掺铥光纤放大器中使用泵浦光功率填充因子大的双包层光纤可以降低光纤长度, 从而减小受激布里渊散射对信号激光输出功率的影响。本文的数值模型可以对光纤放大器的光纤长度进行优化, 对提高实验效率、降低实验成本具有重要价值。

关　键　词: 受激布里渊散射; 双包层; 掺铥光纤; 放大器
中图分类号: O437.2　　**文献标志码:** A　　**doi:** 10.37188/CO.EN-2023-0011

1　Introduction

Fiber lasers are one of the earliest types of realized laser. Initially, most fiber lasers used a single-clad fiber as the laser medium, but it is difficult to effectively couple high power pump wave into the fiber core due to the geometry of the fiber core. Consequently, fiber lasers were formerly regarded as a weak wave source with low output power[1-3]. In 1988, Snitzer *et al.*[4] reported a double-clad fiber, in which, the pump wave is transmitted in the inner cladding, providing a new solution for increasing fiber laser output power, while successfully coupling high-power pump waves into a single-mode core. Double-clad fiber lasers are highly favored by researchers due to their high efficiency, superior mode quality, compact structure, and easy to dissipate heat[5-8].

In recent years, the performance requirements of fiber lasers have increased with the development of fiber optic communication technology. Currently, researchers primarily focus on achieving high power output, narrow linewidth spectrum, and high beam quality in fiber lasers[9-10]. Thulium-doped fiber lasers in the 2 μm band are widely used in laser medicine[11-12], laser active remote sensing[13-14] and military science and technology[15] due to their advantages including human eye safety and wide tunable range. As a result, they have garnered significant attention in the optical society. In recent years, there has been a growing interest in ultrashort pulse and multi-wavelength fiber laser light sources in the 2.0 μm[16-19]. In addition, thulium-doped fiber lasers offer great advantages in terms of a narrow linewidth and high-power laser output[20]. To further improve the laser output wave's beam quality, a Master Oscillation Power Amplification (MOPA) structure is usually used[21]. However, in the high-power fiber amplifiers, the small core cross-sectional area and high transmission power can easily cause nonlinear effects. The Stimulated Brillouin Scattering (SBS) effect[22] can convert part of the signal wave in the amplifer into a Stokes wave, thus affects the efficiency of the amplifier and leads to a significant reduction in the output power[23]. There-

fore, the suppression of SBS in fiber lasers or amplifiers is a very important research topic. For example, Yang L *et al.*[24] broadened the pump wave by using white noise as the RF signal to reduce the Brillouin scattering gain coefficient. As a result, the SBS threshold was increased, and a continuous laser output with an average power of 90 W was achieved. Liu Y K *et al.*[25] reduced the Brillouin gain peak by broadening the linewidth of the seed laser by using phase modulation to suppress SBS. Harish *et al.*[26] suppressed stimulated Brillouin scattering in an erbium-doped optical fiber amplifier for 50-ns-long transform limited signal pulses by employing counter-directional pumping with a pulse burst. Furthermore, the effect of SBS can be reduced by increasing the mode field area of the fiber[27] and increasing the doping concentration of the gain fiber[28].

Numerical modeling was conducted on the double-clad thulium-doped fiber, with reference to GB/T 28 504.2-2021[29]. An investigation was carried out on the optical field distribution, Brillouin gain coefficient, and Brillouin gain spectrum, along with other characteristics of the double-clad thulium-doped fiber at the pump wavelength of 793 nm and the laser waveband of 1.9~2.1 μm. Subsequently, the numeric solution for the laser output characteristics of the thulium-doped fiber amplifier is obtained, considering the effect of SBS on the output power of the signal wave. The results show that the effect of SBS on the signal laser output can be reduced by choosing a shorter fiber in the fiber amplifier, while a double-clad fiber with a larger pump optical power filling factor can be used to guarantee the laser output power.

2 Models and theory

A Double-Clad Thulium-Doped Fiber (DCTDF) has a four-layer structure. The core portion is made of Tm^{3+}-doped silica, with an inner cladding layer of pure silica, an outer cladding layer of a low-refractive index polymer, and a coating layer of a common polymer[29]. For its geometry, optical properties, mechanical properties, and other parameters, please refer to GB/T 28 504.2-2021. The DTDFs can be categorized as DTDF-10/130 and DTDF-25/400 according to the size of their core and inner cladding. Table 1 gives their respective geometry and optical properties.

Tab. 1 Geometry and optical properties of double-clad thulium-doped fibers

Properties	Unit	DTDF-10/130	DTDF-25/400
Core diameter	μm	10.0 ± 1.0	25.0 ± 2.5
Diameter of inner cladding	μm	130.0 ± 3.0	400.0 ± 15.0
Concentricity error of core/internal cladding	μm	⩽ 2.0	⩽ 4.0
Diameter of coating layer	μm	215.0 ± 10.0	550.0 ± 20
Operating wavelength	nm	1900 ~ 2 100	1900 ~ 2 100
Core numerical aperture	——	0.150 ± 0.010	0.090 ± 0.010
Numerical aperture of inner cladding	——	⩾ 0.460	⩾ 0.460

The refractive index of silica is determined using the Sellmeier equation[30]

$$n_{SiO_2}^2 = 1 + \frac{0.696\,166\,3\lambda^2}{\lambda^2 - (0.068\,404\,3)^2} + \frac{0.407\,942\,6\lambda^2}{\lambda^2 - (0.116\,241\,4)^2} + \frac{0.897\,479\lambda^2}{\lambda^2 - (9.896\,161)^2}, \tag{1}$$

where λ represents the wavelength in microns and n_{SiO_2} represents the refractive index of silica.

Figs. 1 and 2 depict the structure and refractive index distribution of DTDF-10/130 and DTDF-25/400 DCTDFs, respectively. In these diagrams, n_1, n_2 and n_3 represent the refractive indices of the core, inner cladding, and outer cladding. It is worth

noting that in both fibers, n_2 represents the refractive index of silica, while n_1 and n_3 can be calculated from the numerical apertures of the core and inner cladding.

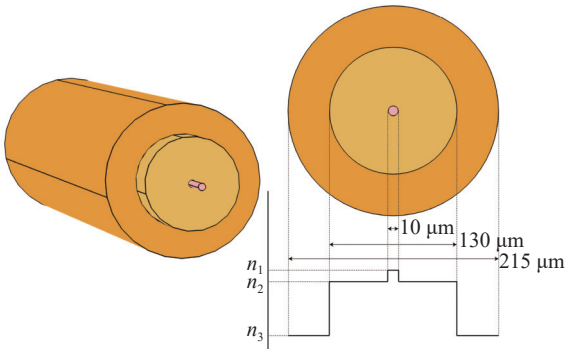

Fig. 1　Structure and refractive index distribution of DTDF-10/130 double-clad thulium-doped fiber

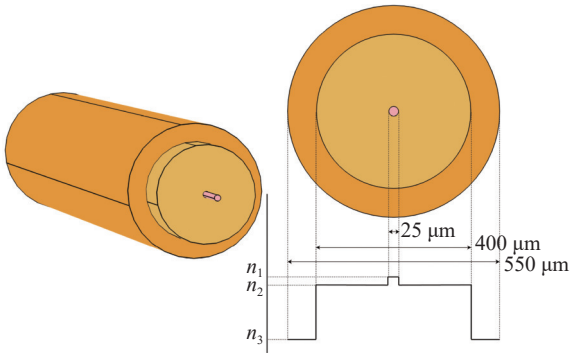

Fig. 2　Structure and refractive index distribution of DTDF-25/400 double-clad thulium-doped fiber

3　Results and discussion

3.1　Analyses of optical properties of double-clad thulium-doped fiber

Analytical calculations were performed using the finite element method for both DTDF-10/130 and DTDF-25/400 DCTDFs. This study focuses on the operating waveband of thulium-doped fiber lasers at 1.9~2.1 μm. The coupling intensity of the optical wave in the Tm^{3+} doped region is quantitatively expressed through the power filling factor shown in the following equation[31-32]

$$\Gamma_k = \frac{\iint\limits_{Tm^{3+}\text{doped}} |E_k(x,y)|^2 \mathrm{d}x\mathrm{d}y}{\iint\limits_{\text{ALL}} |E_k(x,y)|^2 \mathrm{d}x\mathrm{d}y}, \qquad (2)$$

where the integration region of the numerator term is the doping region of Tm^{3+}, while the integration region of the denominator term covers the entire fiber cross section, and k represents various optical modes.

Figs. 3 and 4 show the optical field distributions of the two fibers for the signal wave with a wavelength of 2 μm. As the refractive index of the core-doped region is greater than that of the inner cladding, the signal wave at 2 μm wavelength can be effectively confined in the core-doped region. Fig. 5 (color online) illustrates the normalized frequencies of the two fibers within the signal wave wavelength range of 1.9~2.1 μm. It can be seen from Fig. 5 that the normalized frequency of DTDF-25/400 DCTDF is consistently above 2.405 in this range, indicating that it is a few-mode fiber allowing LP_{01} and LP_{11} modes existence in the core. On the other hand, the normalized frequency of DTDF-10/130 DCTDF surpasses 2.405 only at wavelengths lower than 1.96 μm, suggesting that it maintains single-mode transmission with only LP_{01} mode in the core.

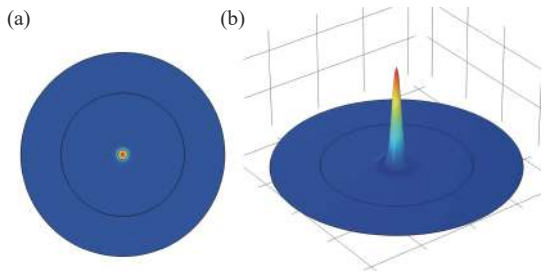

Fig. 3　Schematic diagrams of the (a) two-dimensional and (b) three-dimensional optical field distributions of the LP_{01} mode of the DTDF-10/130 double-clad thulium-doped fiber at 2 μm wavelength, respectively

Figs. 6(a) and (b) (color online) demonstrate the effective refractive index and effective mode field area for LP_{01} mode of DTDF-10/130 DCTDF and LP_{11} mode of DTDF-25/400 DCTDF in the 1.9~2.1 μm signal wave. The plots clearly indicate a positive correlation between the effective mode field area and wavelength. When the signal wave has a wavelength of 2 μm, the effective mode field area

for LP_{01} mode in DTDF-10/130 DCTDF is 94.8 μm^2. For DTDF-25/400 DCTDF, the LP_{01} and LP_{11} modes have effective mode filed areas of 415.5 μm^2 and 677.4 μm^2, respectively. To calculate the power filling factors for both fibers, equation (2) can be used assuming that Tm^{3+} is uniformly doped in the core region. The results are shown in Fig. 7.

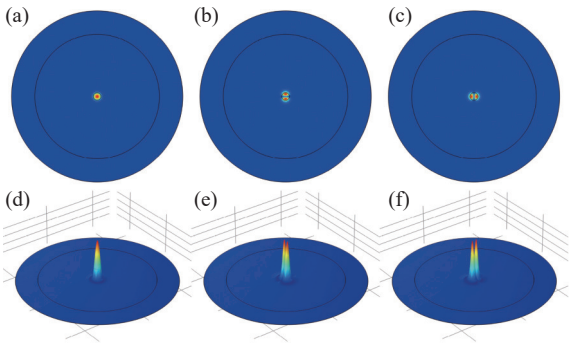

Fig. 4 Optical field distribution of DTDF-25/400 double-clad thulium-doped fiber at 2 μm wavelength. (a)–(c) Schematic diagrams of the two-dimensional optical field distributions for LP_{01}, LP_{11} (o) and LP_{11} (e); (d)–(f) schematic diagrams of three-dimensional optical field distributions for LP_{01}, LP_{11} (o) and LP_{11} (e)

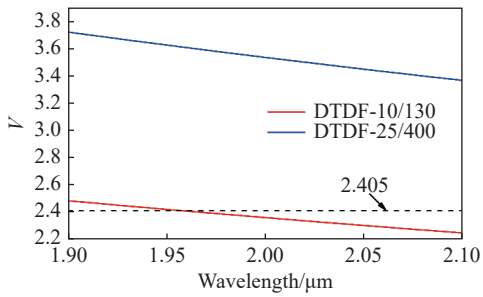

Fig. 5 Schematic diagram of the normalized frequency with signal wave wavelength for DTDF-10/130 and DTDF-25/400 double-clad thulium-doped fibers

In DTDF-10/130 DCTDF, analysis is limited to only the optical power filling factor of LP_{01} mode due to the cutoff of LP_{11} mode for signal wave with wavelength above 1.96 μm. As the wavelength increases from 1.9 μm to 2.1 μm, the optical power filling factor of LP_{01} mode decreases from 0.838 to 0.797. In DTDF-25/400 DCTDF, both LP_{01} and LP_{11} modes exist within the 1.9~2.1 μm signal waveband. As the wavelength increases from 1.9 μm to 2.1 μm, the optical power filling factor of LP_{01} mode decreases from 0.939 to 0.922, while that of LP_{11} mode decreases from 0.815 to 0.754. It is worth noting that the optical power filling factor of LP_{01} mode remains consistently larger than that of LP_{11} mode. Therefore, LP_{01} mode has a stronger Tm^{3+} doping gain capability than LP_{11} mode. This advantages allowed LP_{01} mode to persevere in the mode competition with LP_{11} mode.

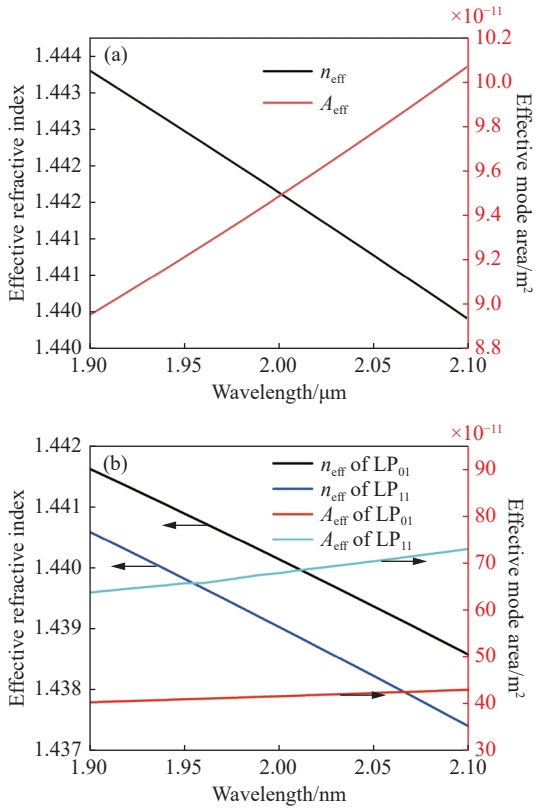

Fig. 6 Effective refractive index and effective mode field area of different optical wave modes in two fibers in the 1.9~2.1 μm band. (a) LP_{01} mode in DTDF-10/130 double-clad thulium-doped fiber; (b) LP_{01} and LP_{11} modes in DTDF-25/400 double-clad thulium-doped fiber

The 793 nm pump wave can be transmitted in the core and cladding. Hence, in this paper, the coupling capability of the 793 nm pump wave in the core region and its transmission characteristics in the inner cladding of DTDF-10/130 and DTDF-25/400 DCTDFs are numerically investigated.

The distribution of the optical modes with higher power filling factors in both fibers at a pump wave wavelength of 793 nm are shown in Fig. 8. Power filling factors of optical modes correspond-

ing to 8(a) to 8(d) are 5.11×10^{-4}, 2.28×10^{-3}, 4.90×10^{-3}, and 3.11×10^{-3}, respectively, while those corresponding to 8(e) to 8(h) are 5.64×10^{-4}, 2.46×10^{-3}, 5.17×10^{-3}, and 7.90×10^{-3}, respectively. These optical modes are generally radially symmetric. The number of optical modes which can be accommodated in the inner cladding of the fiber is much greater than those found in Fig. 8. Additionally, optical modes with lower power filling factor in DTDF-10/130 DCTDF can be seen in Fig. 9, with optical modes in Figs. 9(a) to (c) corresponding to power filling factors of 8.98×10^{-6}, 6.84×10^{-7}, and 7.00×10^{-8}, respectively. These are over two orders of magnitude less than those shown in Fig. 8.

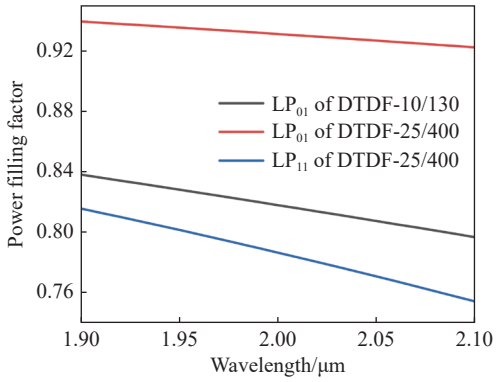

Fig. 7　Variation of power filling factor with wavelength in double-clad thulium-doped fibers DTDF-10/130 and DTDF-25/400

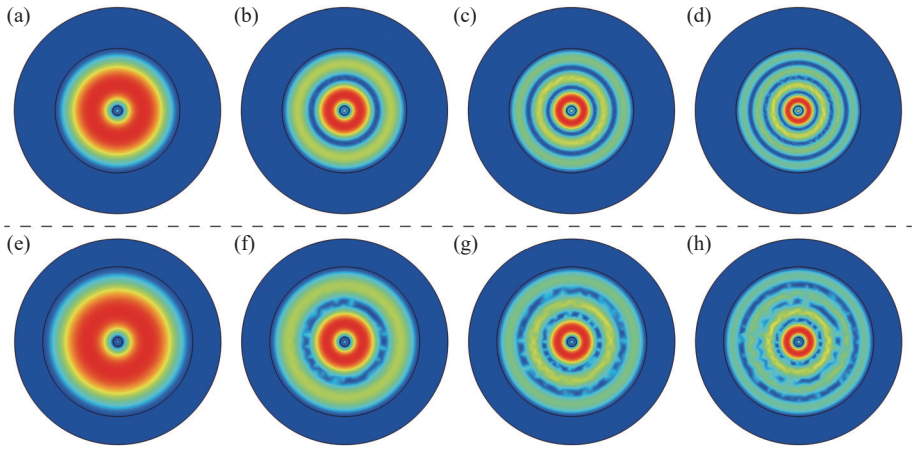

Fig. 8　Optical wave modes of 793 nm pump wave in different fibers. (a)-(d) DTDF-10/130; (e)-(h) DTDF-25/400 double-clad thulium-doped fiber

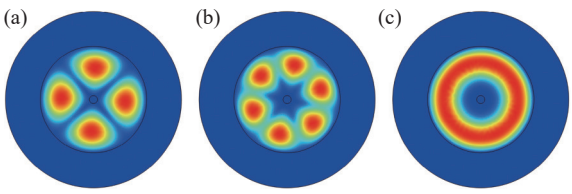

Fig. 9　Optical modes corresponding to small power filling factor in the inner cladding at a wavelength of 793 nm for the pump wave

3.2　Stimulated Brillouin scattering in double-clad thulium-doped fibers

In double-clad thulium-doped fiber application, a 793 nm pump wave is pumped through the cladding, while a laser with a wavelength of 2 μm is amplified and transmitted in the core. The Brillouin scattering threshold is proportional to the effective mode field area, the effective mode field area of the pump wave transmitted in the cladding is significantly greater than that of the laser transmitted in the core. For example, the effective mode field area of the optical wave corresponding to the 793 nm pump wave, as shown in Fig. 8(a), is 8.11×10^{-9} m^2, while that of the LP_{01} mode shown in Fig. 3 at a laser wavelength of 2 μm transmitted in the core is only 9.48×10^{-11} m^2. Consequently, the effective mode field area of the optical mode of the laser is two orders of magnitude smaller than that of the pump wave. Thus, the Brillouin threshold of the pump wave is significantly higher than that of the laser. In the proceeding discussion, we only consider the SBS effect arising in the laser.

The different Brillouin frequency shifts of the two fibers in the laser waveband, ranging from 1.9 to 2.1 μm, can be calculated by equation (2). Fig. 10 depicts a decrease in the Brillouin frequency shift of LP_{01}-LP_{01} intra-mode Brillouin scattering in DTDF-10/130 DCTDF from 8.867 GHz to 8.176 GHz as the laser wavelength increases from 1.9 μm to 2.1 μm. The Brillouin frequency shifts for intra-mode and inter-mode Brillouin scattering in DTDF-25/40 DCTDF have decreased. Specially, the shifts for LP_{01}-LP_{01} intra-mode were from 8.258 GHz to 8.166 GHz, the shifts for LP_{11}-LP_{11} intra-mode were from 8.251 GHz to 8.159 GHz, and the shifts for LP_{01}-LP_{11} inter-mode were from 8.255 GHz to 8.162 GHz.

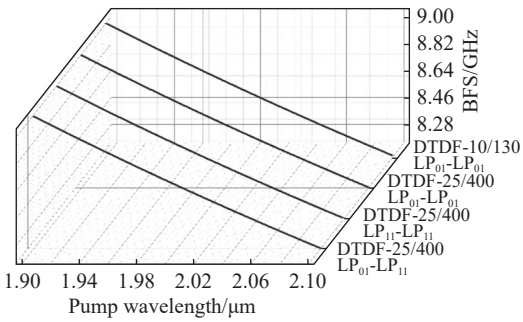

Fig. 10 Schematic diagram of intra- and inter-mode Brillouin scattering of different optical wave modes in two fibers operating at 1.9~2.1 μm laser wave lengths

The Brillouin gain coefficients of LP_{01}-LP_{01} intra-mode Brillouin scattering in DTDF-10/130 DCTDF, LP_{01}-LP_{01} intra-mode, LP_{11}-LP_{11} intra-mode and LP_{01}-LP_{11} inter-mode Brillouin scattering in DTDF-25/400 DCTDF at 1.9~2.1 μm signal waveband are presented in Fig. 11 (color online). The Brillouin gain coefficients in DTDF-10/130 DCTDF are greater than those in DTDF-25/400 DCTDF. While conducting experiments within DTDF-25/400 DCTDF, the Brillouin gain coefficient exhibited the largest value for LP_{01}-LP_{01} intra-mode Brillouin scattering, followed by LP_{11}-LP_{11} intra-mode Brillouin scattering, and ultimately LP_{01}-LP_{11} inter-mode Brillouin scattering, which is the smallest gain coefficient among the three.

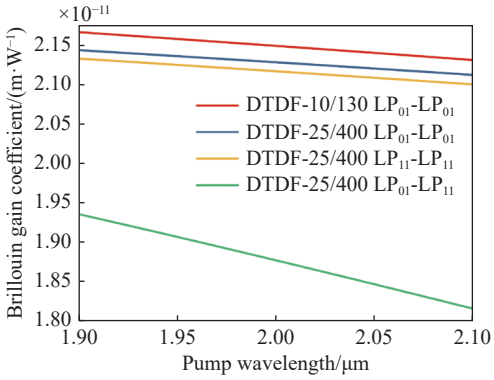

Fig. 11 LP_{01}-LP_{01} intra-mode Brillouin gain coefficient in DTDF-10/130 double-clad thulium-doped fiber, LP_{01}-LP_{01} intra-mode, LP_{11}-LP_{11} intra-mode and LP_{01}-LP_{11} inter-mode Brillouin gain coefficients in DTDF-25/400 double-clad thulium-doped fiber at the 1.9~2.1 μm laser waveband

According to Fig. 5, it can be observed that DTDF-10/130 DCTDF is a single-mode fiber at a laser wavelength of 2 μm, while DTDF-25/400 DCTDF is a few-mode fiber. Therefore, only intra-mode Brillouin scattering is present in DTDF-10/130 DCTDF and its Brillouin gain spectrum is shown in Fig. 12(a). The Brillouin frequency shift is observed to be 8.595 GHz and the Brillouin gain coefficient is determined to be 2.149×10^{-11} m/W. In DTDF-25/400 DCTDF, both LP_{01} and LP_{11} modes exist, and intra-mode Brillouin scattering and inter-mode Brillouin scattering can exist. The Brillouin gain spectrum is shown in Fig. 12(b) (color online), where the Brillouin frequency shifts and the Brillouin gain coefficients of LP_{01}-LP_{01} intra-mode, LP_{11}-LP_{11} intra-mode and LP_{01}-LP_{11} inter-mode Brillouin scattering are 8.583 GHz, 8.577 GHz and 8.580 GHz, and 2.129×10^{-11} m/W, 2.117×10^{-11} m/W, and 1.8×10^{-11} m/W, respectively.

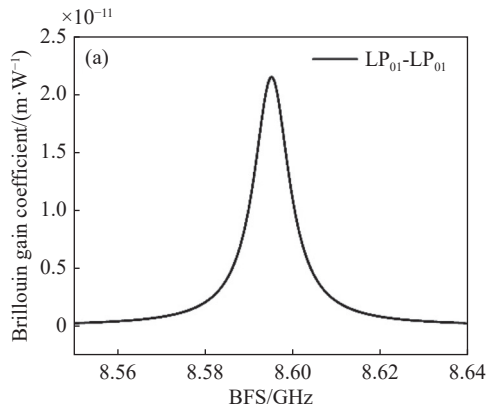

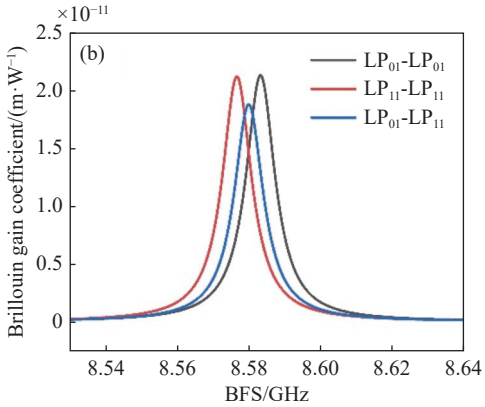

Fig. 12　Brillouin gain spectra at laser wavelength of 2 μm. (a) Brillouin scattering within LP_{01}-LP_{01} mode in DTDF-10/130 double-clad thulium-doped fiber; (b) Brillouin scattering within LP_{01}-LP_{01} mode, LP_{11}-LP_{11} mode and LP_{01}-LP_{11} inter-mode in DTDF-25/400 double-clad thulium-doped fiber

3.3　Stimulated Brillouin scattering in thulium-doped fiber amplifiers

The laser in the 2 μm band can be generated or amplified by a DCTDF, which corresponds to a thulium-doped fiber laser and an amplifier respectively. In this paper, we mainly study the SBS in DTDF-10/130 DCTDF amplifier, whose simulation parameters are shown in Table 2[33-35].

The effect of SBS on the output power of the signal wave was simulated in a DCTDF amplifier with pump wave power filling factors of 0.01, 0.02 and 0.03. The seed wave was a continuous wave with a wavelength of 2 μm and a power of 0.01 W, while the pump wave was a continuous wave with a wavelength of 793 nm and a power of 100 W, respectively.

Tab. 2　Simulation parameters of thulium-doped fiber amplifier

Parameter	Symbol	Value	Unit
Fiber core diameter	a	10.0	μm
Inner cladding diameter	b	130.0	μm
Tm^{3+} doping concentration	N_0	5.5×10^{25}	m^{-3}
Pump wavelength	λ_p	793	nm
Signal wave wavelength	λ_s	2	μm
Pump wave absorption cross section	$\sigma_a(\lambda_p)$	8.5×10^{-25}	m^2
Pump wave emission cross section	$\sigma_e(\lambda_p)$	8.9×10^{-25}	m^2
Signal wave absorption cross section	$\sigma_a(\lambda_s)$	0.1×10^{-25}	m^2
Signal wave emission cross section	$\sigma_e(\lambda_s)$	6.2×10^{-25}	m^2
Stimulated Brillouin scattering gain	g_B	2.803×10^{-11}	m/W
Brillouin noise	I_{SBS}	3.350×10^{-7}	W
Pumped optical fiber loss	α_p	1.2×10^{-2}	m^{-1}
Signal optical fiber loss	α_s	2.3×10^{-3}	m^{-1}
Pump optical power filling factor	Γ_p	Influenced by the shape of the inner cladding	-
Signal optical power filling factor	Γ_s	0.817	-

The distribution of pump wave, signal wave, and Stokes wave power along a 2.1 m DTDF-10/130 DCTDF with a pump wave power filling factor of 0.02 is shown in Fig. 13 (color online). The direction of forward wave propagation is specified as the direction of increasing fiber length. The pump wave travels forward and is absorbed by the doped Tm^{3+} in the core, resulting in a gradual decrease in

intensity as fiber length increases. This process excites the Tm^{3+} to the upper energy level of the laser. The signal wave is continuously amplified during transimission process, and when the power of signal wave reaches the SBS threshold, a portion of its energy can be converted into the backward transmitted Stokes wave by SBS. As the SBS process continues, the backward transmitted Stokes wave undergoes gradual amplification. As the transmission direction of the Stokes wave is opposite to that of the signal wave. Fig. 13 illustrates a gradual decrease in the power of the former Stokes wave as the fiber length increases. To maintain optimal output power of the signal wave, suppression of SBS in thulium-doped fiber amplifiers is required.

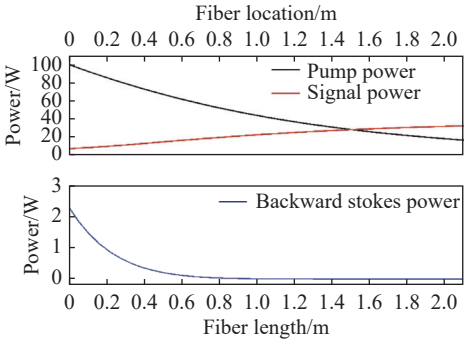

Fig. 13 Distribution of pump wave power, signal wave power and Stokes wave power along the fiber

In this paper, we investigate how fiber length affects the output power of a thulium-doped fiber amplifier. First, the effect of fiber length on the pump wave absorption is studied, and the results are shown in Fig. 14 (color online). It can be seen that as fiber length increases, the power of pump wave which is not absorbed by Tm^{3+} decreases gradually. Therefore, a shorter fiber length is required to absorb the same power of pump wave for a DCTDF with a larger power filling factor. For example, when 80% of the pump wave is absorbed, the lengths of DCTDFs with pump wave power filling factors of 0.01, 0.02 and 0.03 need to be approximately about 3.6 m, 1.9 m and 1.3 m, respectively.

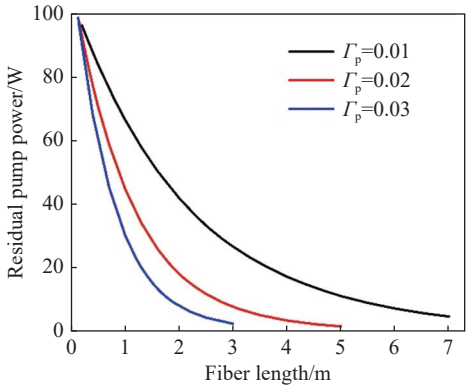

Fig. 14 Residual pumping optical powers varying with fiber length at different pump optical power filling factors

As shown in Fig. 15 (color online), the 2 μm laser achieves a maximum output power of 25.27 W, 31.08 W and 34.06 W when the pump optical power filling factors are 0.01, 0.02 and 0.03, respectively. The corresponding fiber lengths are 2.66 m, 2.02 m and 1.75 m. The reverse transmitted Stokes optical power caused by SBS is 1.68 W, 1.39 W and 1.14 W, respectively. The laser output power increases and then decreases as the fiber length increases, while the Stokes power for reverse transmission continues to increase, as shown in the figure 15. Therefore, effective laser amplification can be realized by selecting a shorter fiber and a DCTDF with a larger pump power filling factor as the gain medium to suppress the SBS. To this end, the pump power filling factor can be optimized by the rational design of the inner cladding structure.

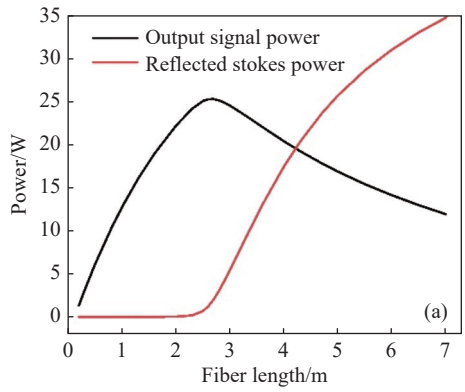

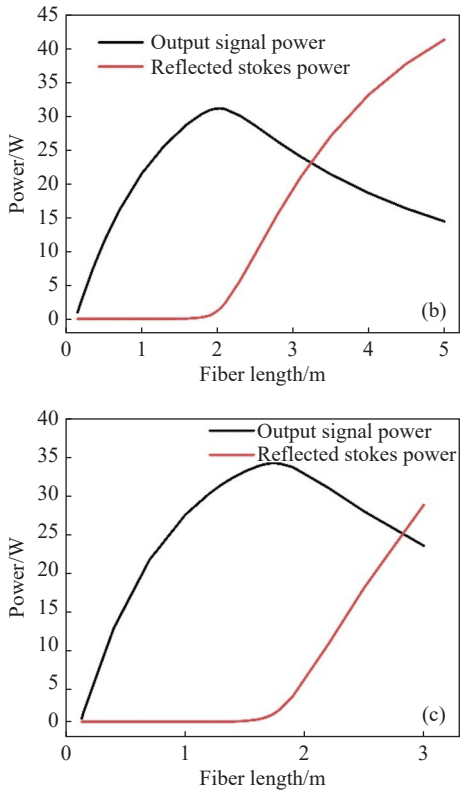

Fig. 15　Variation of laser output power and Stokes optical power with fiber length when pump power filling factors are (a) 0.01, (b) 0.02, and (c) 0.03, respectively

4　Conclusion

Compared to DTDF-25/400 double-clad thulium-doped fiber, DTDF-10/130 double-clad thulium-doped fiber can maintain single-mode transmission at 793 nm pump wavelength in the laser waveband of 1.9~2.1 μm. Only the SBS of the signal wave in the core was investigated in both fibers since the pump's Brillouin threshold is considerably larger than that of the signal wave. The study indicates the presence of both intra- and inter-mode Brillouin scattering in DTDF-25/400 as the signal wavelength increases from 1.9 μm to 2.1 μm. On the other hand, only intra-mode Brillouin scattering is observed in DTDF-10/130. For DTDF-10/130 double-clad thulium-doped fiber amplifier with varying pump wave power filling factors of 0.01, 0.02 and 0.03, by using 100 W continuous wave with wavelength of 793 nm as the pump wave and 0.01 W continuous wave wavelength of 2 μm as the signal wave, the maximum output power of the signal wave is 25.27 W, 31.08 W and 34.06 W, respectively. The optimal double-clad fiber lengths are 2.66 m, 2.02 m and 1.75 m, respectively. The Stokes optical power generated by stimulated Brillouin scattering is 1.68 W, 1.39 W and 1.14 W. The results show that using double-clad fiber with a high pump power filling factor in the thulium-doped fiber amplifier can minimize the effects of stimulated Brillouin scattering on the signal laser output power by reducing the fiber length. The numerical model presented in this paper optimizes the fiber length of the fiber amplifier. This optimization is significant in improving experimental efficiency and reducing experimental costs.

References:

[1]　姚建铨, 任广军, 张强, 等. 掺镱双包层光纤激光器及其泵浦耦合技术[J]. 激光杂志, 2006, 27(5): 1-4.
YAO J Q, REN G J, ZHANG Q, *et al*.. Ytterbium-doped double clad fiber laser and pump coupling technology[J]. *Laser Journal*, 2006, 27(5): 1-4. (in Chinese).

[2]　刘伟伟, 宋峰, 李加, 等. 包层泵浦上转换光纤激光器进展[J]. 激光杂志, 2000, 21(1): 10-12.
LIU W W, SONG F, LI J, *et al*.. Cladding pumping upconversion fiber laser[J]. *Laser Journal*, 2000, 21(1): 10-12. (in Chinese).

[3]　刘强, 杨仕平, 雷菁. 包层泵浦光纤激光器及应用[J]. 光通信技术, 2005, 29(6): 54-56.
LIU Q, YANG SH P, LEI J. Cladding pump fiber lasers and its application[J]. *Optical Communication Technology*, 2005, 29(6): 54-56. (in Chinese).

[4]　SNITZER E, PO H, HAKIMI F, *et al*. . Double clad, offset core Nd fiber laser[C]. *Optical Fiber Sensors 1988*, Optica Publishing Group, 1988.

[5]　ZHANG H R, ZHANG J J, SUN SH ZH, *et al*.. Self-mode-locking and self-phase modulation in Tm^{3+}-doped double clad fiber laser for pulse peak power enhancement and multi-wavelength generation[J]. *Optics & Laser Technology*, 2021,

141: 107128.

[6] DURÁN-SÁNCHEZ M, POSADA-RAMÍREZ B, ÁLVAREZ-TAMAYO R I, *et al*.. Low repetition rate gain-switched double-clad thulium-doped fiber laser operating in the 2μm wavelength region[J]. *Optical Fiber Technology*, 2021, 66: 102660.

[7] 沈永行, 吴波, 胡澄之, 等. 激光差频技术实现高平均功率 3.8μm 纳秒中波红外激光输出实验研究[J]. 中国激光, 2022, 49(1): 0101017.
SHEN Y H, WU B, HU CH ZH, *et al*.. Experimental investigation on the high average power ns mid-infrared laser output at 3.8μm through difference frequency generation[J]. *Chinese Journal of Lasers*, 2022, 49(1): 0101017. (in Chinese).

[8] ZHONG P L, WANG L, YANG B L, *et al*.. 2 × 2kW near-single-mode bidirectional high-power output from a single-cavity monolithic fiber laser[J]. *Optics Letters*, 2022, 47(11): 2806-2809.

[9] HUANG ZH M, SHU Q, TAO R M, *et al*.. >5kW record high power narrow linewidth laser from traditional step-index monolithic fiber amplifier[J]. *IEEE Photonics Technology Letters*, 2021, 33(21): 1181-1184.

[10] XU Y, SHENG Q, WANG P, *et al*. . 1. 5-kW all-fiberized Yb-doped MOPA laser at 1105nm with near-diffraction-limited beam quality and narrow spectral width[J]. *Optics Communications*, 2022, 511: 127893.

[11] 张安军, 段嘉霖, 邢颖滨, 等. 掺铥激光在生物医疗领域的应用[J]. 激光与光电子学进展, 2022, 59(1): 0100004.
ZHANG A J, DUAN J L, XING Y B, *et al*.. Application of thulium-doped laser in the biomedicine field[J]. *Laser & Optoelectronics Progress*, 2022, 59(1): 0100004. (in Chinese).

[12] 陈忆兰, 朱小磊, 张俊旋, 等. 单频 2μm 波段全固态脉冲激光器技术进展[J]. 激光与光电子学进展, 2020, 57(5): 050006.
CHEN Y L, ZHU X L, ZHANG J X, *et al*.. Development of pulsed single-frequency 2μm all-solid-state laser[J]. *Laser & Optoelectronics Progress*, 2020, 57(5): 050006. (in Chinese).

[13] SINGH U N, KAVAYA M, KOCH G, *et al*.. Solid-state 2-micron laser transmitter advancement for wind and carbon dioxide measurements from ground, airborne, and space-based lidar systems[J]. *Proceedings of SPIE*, 2008, 7111: 711104.

[14] SINGH U N, WALSH B M, YU J R, *et al*.. Twenty years of Tm: Ho: YLF and LuLiF laser development for global wind and carbon dioxide active remote sensing[J]. *Optical Materials Express*, 2015, 5(4): 827-837.

[15] WULFMEYER V, RANDALL M, BREWER A, *et al*.. 2-μm Doppler lidar transmitter with high frequency stability and low chirp[J]. *Optics Letters*, 2000, 25(17): 1228-1230.

[16] ISHII S, MIZUTANI K, IWAI H, *et al*. . 2-μm coherent lidar technology developed at NICT: past, current, and future[C]. *Applications of Lasers for Sensing and Free Space Communications 2015*, Optica Publishing Group, 2015.

[17] WANG X F, WANG J, DUAN X Y. Experimental investigation on evolution of a split multi-wavelength bright-dark pulse in a mode-locked thulium-doped fiber laser[J]. *Optoelectronics Letters*, 2022, 18(12): 717-722.

[18] 宋伟华, 彭志刚, 侯玉斌, 等. 高功率 2 μm 波长可调谐超短脉冲光纤激光器[J]. 强激光与粒子束, 2022, 34(3): 031002.
SONG W H, PENG ZH G, HOU Y B, *et al*.. High-power wavelength-tunable ultrashort pulse firer laser at 2 μm[J]. *High Power Laser and Particle Beams*, 2022, 34(3): 031002. (in Chinese).

[19] YING G, FENG P Y, TING F, *et al*.. Wavelength-interval-switchable multi-wavelength thulium-doped fiber laser with a nonlinear dual-pass Mach-Zehnder interferometer filter in 2-μm-band[J]. *Optics & Laser Technology*, 2022, 145: 107470.

[20] GUAN B, YAN F P, YANG D D, *et al*.. Sub-kHz narrow-linewidth single-longitudinal-mode thulium-doped fiber laser utilizing triple-coupler ring-based compound-cavity filter[J]. *Photonics*, 2023, 10(2): 209.

[21] 杨保来, 杨欢, 叶云, 等. 国产纺锤形渐变掺镱光纤实现 6 kW 宽谱激光输出[J]. 强激光与粒子束, 2022, 34(8): 081001.
YANG B L, YAGN H, YE Y, *et al*.. 6 kW broadband fiber laser based on home-made ytterbium-doped fiber with gradually varying spindle-shape structure[J]. *High Power Laser and Particle Beams*, 2022, 34(8): 081001. (in Chinese).

[22] LIU CH, LIU J, ZHANG Y J, *et al*.. Stimulated Brillouin scattering suppression of thulium-doped fiber amplifier with fiber superfluorescent seed source[J]. *Optics Express*, 2017, 25(9): 9569-9578.

[23] KOVALEV V I, HARRISON R G, NILSSON J, *et al*.. Analytic modeling of Brillouin gain in rare-earth doped fiber amplifiers with high-power single-frequency signals[J]. *Proceedings of SPIE*, 2005, 5709: 142-146.

[24] 杨磊, 郑加金, 郝丽云, 等. 信号光谱宽特性对单频光纤放大器 SBS 阈值的影响[J]. 中国激光, 2017, 44(9): 0901009.
YANG L, ZHENG J J, HAO L Y, *et al*.. Influence of signal spectral width characteristic on SBS threshold of single frequency fiber amplifier[J]. *Chinese Journal of Lasers*, 2017, 44(9): 0901009. (in Chinese).

[25] 刘雅坤, 王小林, 粟荣涛, 等. 相位调制信号对窄线宽光纤放大器线宽特性和受激布里渊散射阈值的影响[J]. 物理学报, 2017, 66(23): 234203.
LIU Y K, WANG X L, SU R T, *et al*.. Effect of phase modulation on linewidth and stimulated Brillouin scattering threshold of narrow-linewidth fiber amplifiers[J]. *Acta Physica Sinica*, 2017, 66(23): 234203. (in Chinese).

[26] HARISH A V, NILSSON J. Suppression of stimulated Brillouin scattering in pulsed erbium-doped fiber amplifier through intensity-modulated counter pumping[J]. *Optical Engineering*, 2019, 58(10): 102703.

[27] HUANG B, WANG J Q, SHAO X P. Fiber-based techniques to suppress stimulated brillouin scattering[J]. *Photonics*, 2023, 10(3): 282.

[28] 田浩, 史朝督, 付士杰, 等. 0.59 mJ 单频掺 Yb3+百纳秒脉冲全光纤激光器[J]. 中国激光, 2022, 49(13): 1301005.
TIAN H, SHI CH D, FU SH J, *et al*.. 0.59-mJ single-frequency Yb-$^{3+}$-doped hundred-nanosecond pulsed all-fiber laser[J]. *Chinese Journal of Lasers*, 2022, 49(13): 1301005. (in Chinese).

[29] 全国通信标准化技术委员会. GB/T 28504.2-2021 掺稀土光纤 第 2 部分: 双包层掺铥光纤特性[S]. 北京: 中国标准出版社, 2021.
National Communications Standardization Technical Committee. GB/T 28504.2-2021 Rare earth doped optical fibre—Part 2: Characteristics of double-cladding thulium-doped optical fibre[S]. Beijing: Standards Press of China, 2021. (in Chinese).

[30] LIU Q M, CHEN J P, HOU SH L, *et al*.. Investigation into micro-polishing photonic crystal fibers for surface plasmon resonance sensing[J]. *Crystals*, 2022, 12(8): 1106.

[31] GILES C R, DESURVIRE E. Modeling erbium-doped fiber amplifiers[J]. *Journal of Lightwave Technology*, 1991, 9(2): 271-283.

[32] HUANG L J, YAO T F, YANG B H, *et al*.. Modified single trench fiber with effective single-mode operation for high-power application[J]. *IEEE Journal of Selected Topics in Quantum Electronics*, 2018, 24(3): 0901409.

[33] JACKSON S D, KING T A. Theoretical modeling of Tm-doped silica fiber lasers[J]. *Journal of Lightwave Technology*, 1999, 17(5): 948-956.

[34] SHEN X, ZHOU J H, YANG G L, *et al*.. Temperature characteristics analysis of a Tm^{3+}-doped heterogeneous helical cladding fiber amplifier[J]. *Applied Physics B*, 2022, 128(12): 221.

[35] FANG Q, SHI W, KIEU K, *et al*.. High power and high energy monolithic single frequency 2 μm nanosecond pulsed fiber laser by using large core Tm^{3+}-doped germanate fibers: experiment and modeling[J]. *Optics Express*, 2012, 20(15): 16410-16420.

Author Biographics:

LIU Qing-min (1993—), female, born in Fuyang, Anhui Province, China, received her M.S. degree from Lanzhou University of Technology in 2022. Her research area is primarily focused on fiber optic sensing. E-mail: Celina1026@163.com

HOU Shang-lin (1970—), male, born in Qin'an, Gansu Province, Professor, received his PhD from Beijing University of Posts and Telecommunications in 2008. His research predominantly focuses on developing new optical fiber and high-speed optical communication devices, next-generation high-speed all-optical communication networks, and optical fiber sensor devices and networks. E-mail: houshanglin@vip.163.com